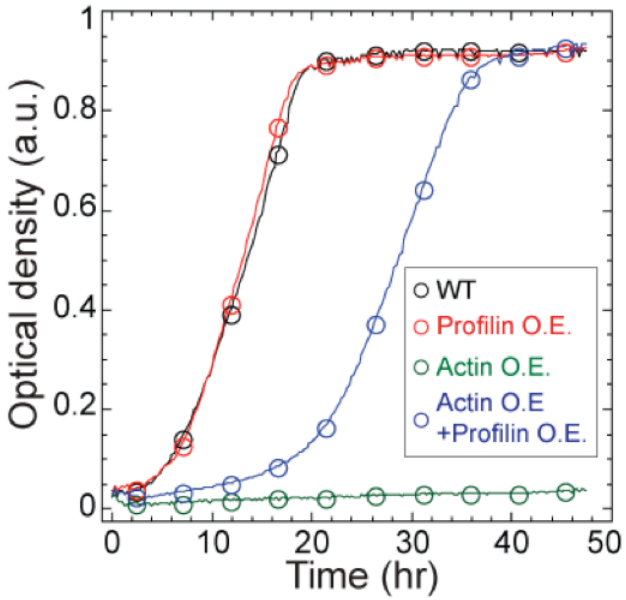


**Figure S1. Over-expressing profilin rescues growth defects caused by over-expressing actin, related to Figure 1**

Plot of the optical density (growth) of fission yeast over time for WT cells (black), cells over-expressing (O.E.) profilin (red), cells O.E. actin (green), or cells O.E. both actin and profilin (blue). Optical density readings were initiated 8 hours after over-expression was initiated by washing cells in EMM5S minimal growth media without thiamine.

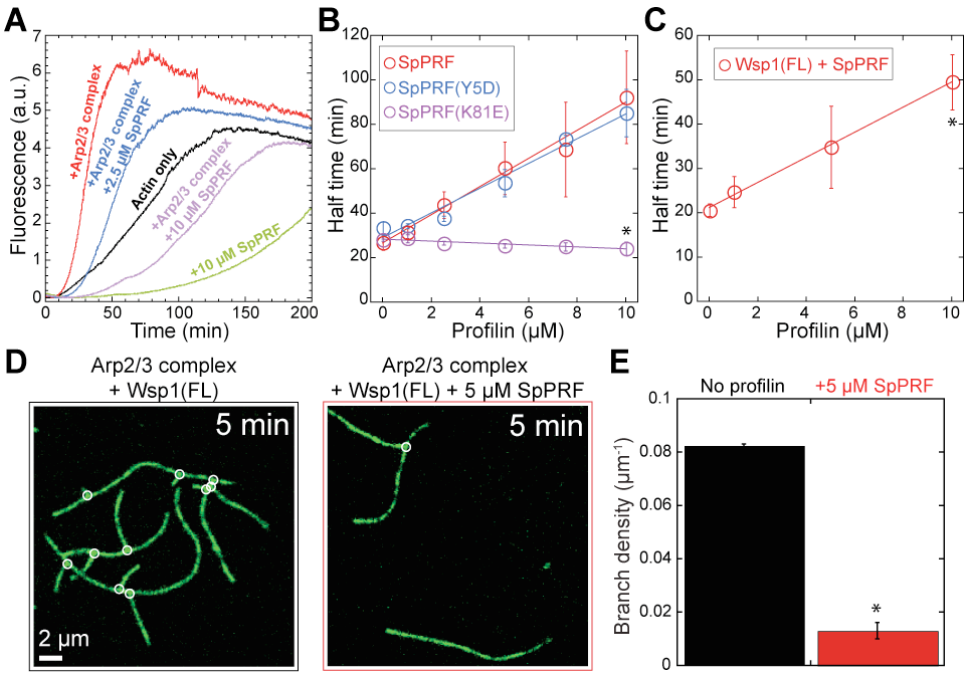


**Figure S2. Profilin inhibits Arp2/3 complex-mediated actin assembly *in vitro*, related to Figure 3.**

(A-C) Pyrene assays: polymerization of 1.0 μM Mg-ATP-actin monomers (20% pyrene-actin) with (A and B) 25 nM SpArp2/3 complex and 100 nM SpWsp1(VCA) or (C) 50 nM SpArp2/3 complex and 50 nM SpWsp1(FL).

(A) Time course of actin only (black) or with 10 μM WT profilin SpPRF (green), actin with SpArp2/3 complex and SpWsp1(VCA) (red), and actin with SpArp2/3 complex and SpWsp1(VCA) and 2.5 (blue) or 10 μM SpPRF (purple).

(B) Plot of the dependence of the time to half-maximal polymerization on the concentration of WT SpPRF (red), SpPRF(Y5D) (blue) or SpPRF(K81E) (purple). Error bars, s.e.; n=2 reactions. Asterisk indicates statistical significance, T-test: * $p<0.04$.

(C) Plot of the dependence of the time to half-maximal polymerization on the concentration of WT SpPRF. Error bars, s.e.; n=2 reactions. Asterisk indicates statistical significance in the absence and presence of 10 μM SpPRF, T-test: * $p<0.05$.

(D and E) TIRFM visualization of 1.5 μM Mg-ATP-actin (15% Oregon Green-actin) with 40 nM SpArp2/3 complex and 60 nM SpWsp1(FL), in the absence and presence of 5 μM WT SpPRF.

(D) Fluorescent micrographs of TIRFM reactions after five minutes.

(E) Arp2/3 complex branch density in the absence and presence of SpPRF. Error bars, s.e.; n=2 reactions. Asterisk indicates statistical significance, T-test: * $p<0.005$.

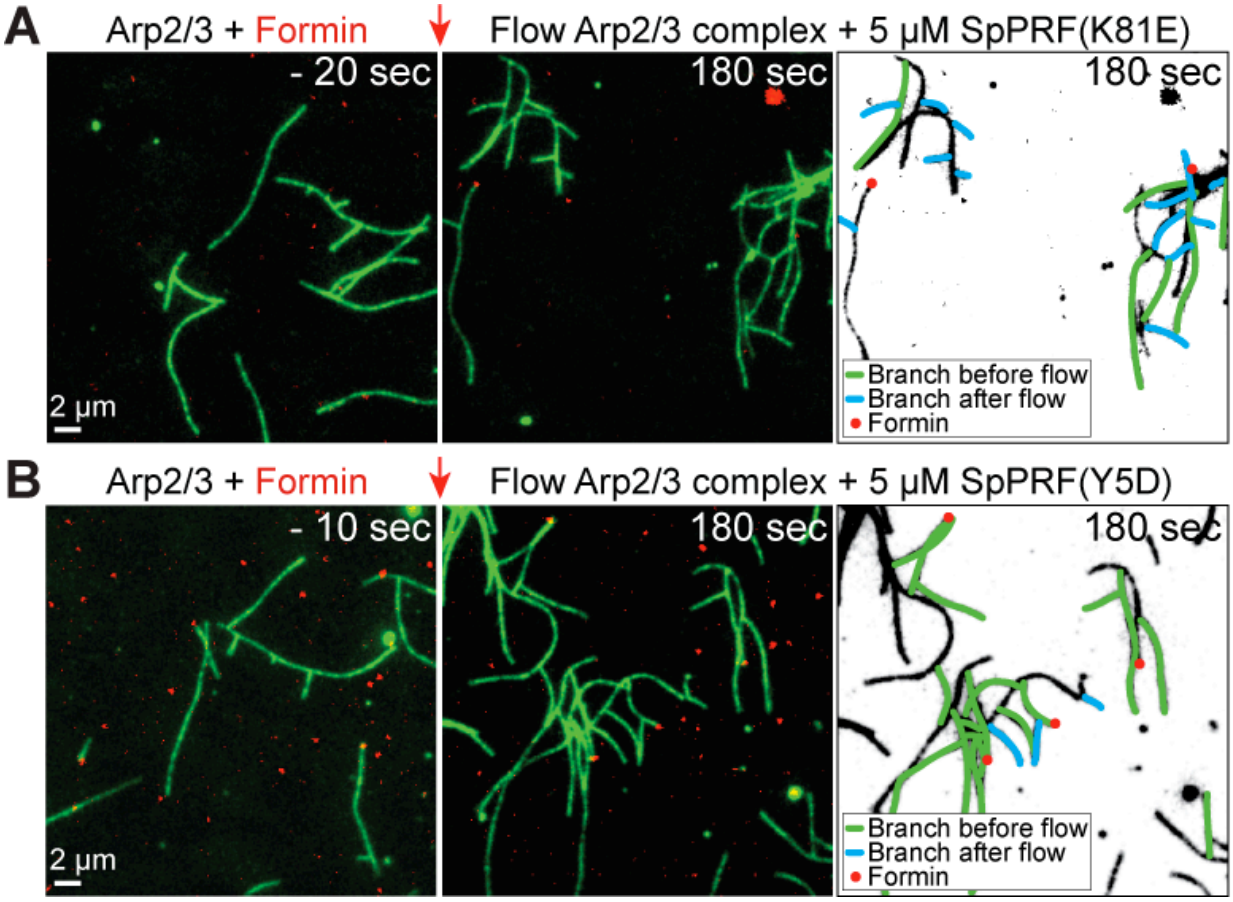


**Figure S3. Flow of mutant profilins into reactions containing mixtures of Arp2/3 complex and formin, related to Figure 4.**

TIRFM visualization of 1.5 µM Mg-ATP-actin (15% Oregon Green-actin) with 40 nM SpArp2/3 complex, 80 nM SpWsp1(VCA), 10 pM formin SNAP-549(red)-SpCdc12(FH1$^{1P}$FH2), and 5 µM profilin mutants (A) SpPRF(K81E) or (B) SpPRF(Y5D). Initial reactions contained Mg-ATP-actin, Arp2/3 complex, SpWsp1(VCA) and formin. At t=0 sec (red arrow) additional Mg-ATP-actin, Arp2/3 complex and SpWsp1(VCA) were flowed into the chamber with profilin. In the inverted micrograph at 180 sec, formin (red dots), and Arp2/3 complex branches initiated before (green) and after (blue) flow are marked. Plots of the dependence of branch density and length of total formin-associated F-actin mass over time are shown in Figures 4C and 4D.

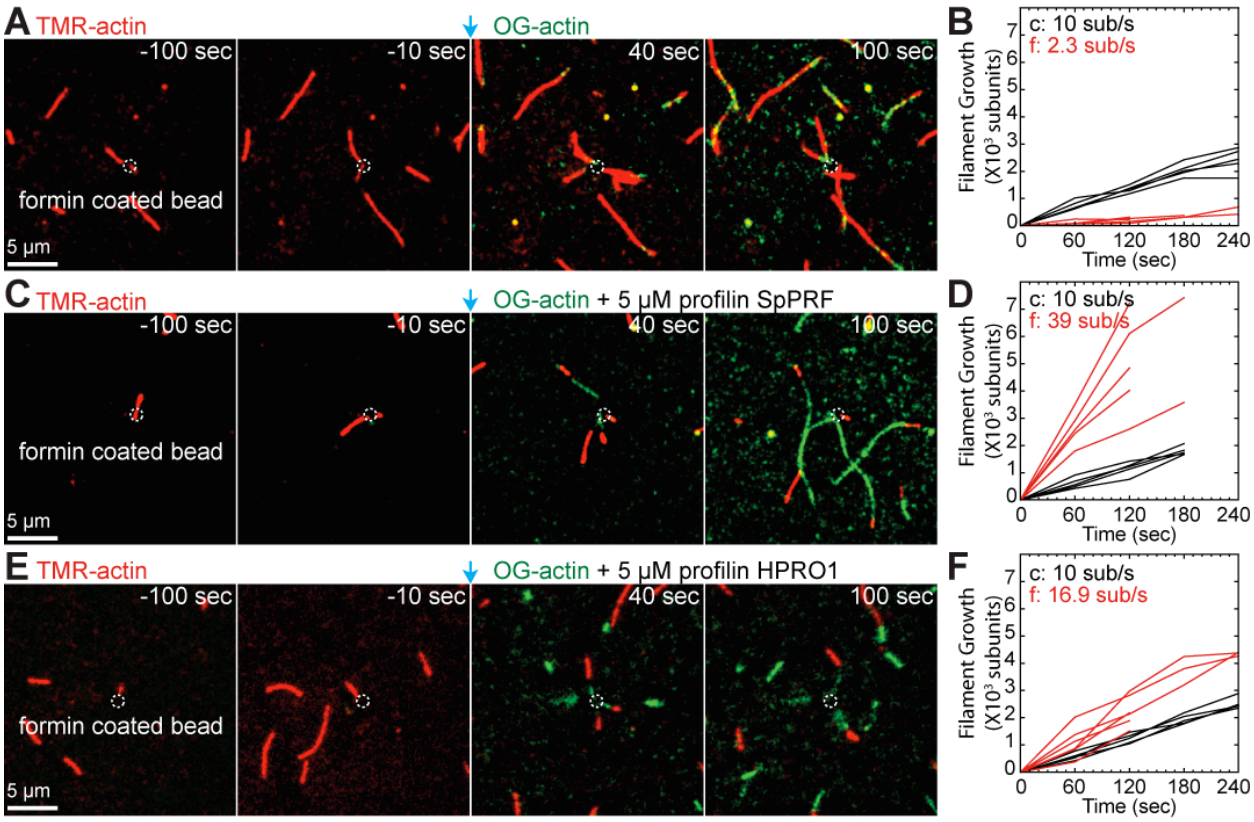


**Figure S4. Biomimetic reconstitution of the effect of profilin on formin-mediated F-actin network formation, related to Figure 5.**

(A–F) TIRFM visualization of the assembly of 1.5 µM Mg-ATP-actin monomers from beads coated with formin SNAP-mDia2(FH1FH2) (dashed circle). Initial reactions contained 10% TMR(red)-actin. At t=0 sec (blue arrow) 15% Oregon green-actin was flowed into the reaction chamber in the absence (A, B) and presence of 5 µM profilin SpPRF (C, D) or HPRO1 (E, F).

(A, C, E) Fluorescent micrographs of the time series.

(B, D, F) Plot of individual filament lengths over time, revealing average elongation rates for control (c) and formin-associated (f) filaments. n=5 filaments. SNAP-mDia2(FH1FH2)-assembled filaments elongate 4-fold slower than control filaments in the absence of profilin, whereas they elongate ~4- and ~2-fold faster than control filaments in the presence of profilins SpPRF or HPRO1.

## SUPPLEMENTAL TABLES

**Table S1: Inhibition of Arp2/3 complex only suppresses cytokinesis defects in profilin mutant cells, related to Figure 6.**

| Strain | Cells with ≥2 nuclei | Cells with abnormal septa | Cells with ≥2 nuclei | Cells with abnormal septa | Cells with ≥2 nuclei | Cells with abnormal septa | Cells with ≥2 nuclei | Cells with abnormal septa |
|---|---|---|---|---|---|---|---|---|
| | DMSO, 25˚C | | CK-666, 25˚C | | DMSO, 33.5˚C | | CK-666, 33.5˚C | |
| *cdc3-124* | 29 | 6 | 14 | 37 | 88 | 92 | 45 | 60 |
| *cdc8-27* | 23 | 7 | 12 | 18 | 91 | 94 | 93 | 94 |
| *cdc4-8* | 22 | 10 | 22 | 5 | 93 | 80 | 89 | 96 |
| *cdc12-112* | 24 | 3 | 20 | 9 | 86 | 95 | 92 | 93 |

**Table S1. Inhibition of Arp2/3 complex only suppresses cytokinesis defects in profilin mutant cells, related to Figure 6.** Cells were incubated in the absence (DMSO) and presence of 50 μM Arp2/3 complex inhibitor CK-666 for four hours at 25 or 33.5°C. All values are percent of scored cells, n≥200 cells for nuclei and n≥28 cells for septa: profilin mutant *cdc3-124*, tropomyosin mutant *cdc8-27*, myosin II essential light chain mutant *cdc4-8*, and cytokinesis formin mutant *cdc12-112*.

**Table S2: Fission yeast strains used in this study, related to Experimental Procedures.**

| Strain name | Genotype | Reference |
|---|---|---|
| MBY6844 | *h-, pAct1 Lifeact-mCherry::Leu+; ade6-m216; leu1-32; ura4-D18* | (Huang et al., 2012) |
| KV624 | *h+, cdc3-124, pAct1-Lifeact-mCherry::Leu1+, leu1-32, ura4-D18, ade6-M216* | This study |
| KV653 | *h?, cdc3-124, pAct1-Lifeact-mCherry::Leu1+, Pnmt81-SpPRF::Ura4+, ura4-294, leu1-32* | This study |
| KV703 | *h?, cdc3-124, pAct1-Lifeact-mCherry::Leu1+, Pnmt81-SpPRF(Y5D)::Ura4+, ura4-294, leu1-32* | This study |
| KV704 | *h?, cdc3-124, pAct1-Lifeact-mCherry::Leu1+, Pnmt81-SpPRF(K81E)::Ura4+, ura4-294, leu1-32* | This study |
| KV354 | *h-, rlc1-GFP-KanMX6, leu1-32, ura4-D18, ade6-M216* | (Lord and Pollard, 2004) |
| KV614 | *h+, cdc3-124, rlc1-GFP-KanMX6, leu1-32, ura4-D18, ade6-M216* | This study |
| KV643 | *h?, cdc3-124, rlc1-GFP-KanMX6, Pnmt81-SpPRF::Ura4+, ura4-294* | This study |
| KV701 | *h?, cdc3-124, rlc1-GFP-KanMX6, Pnmt81-SpPRF(Y5D)::Ura4+, ura4-294* | This study |
| KV702 | *h?, cdc3-124, rlc1-GFP-KanMX6, Pnmt81-SpPRF(K81E)::Ura4+, ura4-294* | This study |
| JW21 | *h-, cdc4-8, his7-366, leu1-32, ura4-D18, ade6-M216* | (McCollum et al., 1995; Nurse et al., 1976) |
| FC20 | *h-, cdc12-112, his7-366, ura4-D18, leu1-32, ade6-M216* | (Chang et al., 1997) |
| TP9 | *h-, cdc8-27, his7-366, ura4-D18, leu1-32, ade6-M216* | (Kovar et al., 2005) |
| KV695 | *h?, cdc3-124, acp2-GFP::kanMX6, his7-366, leu1-32, ura4-D18, ade6-216* | This study |
| VS1590-5B | *h-, Lifeact-GFP::Leu+, act1::KanMX6-3xPnmt1-act1, ade6+, ura4-D18, his3-D1, leu1-32* | (Burke et al., 2014) |
| VS1664-10A | *h- ade6-M210 ura4-D18 his3-D1 natMX4-3xPnmt1-cdc3 leu1-32::Pact1-LifeAct-GFP-leu1+* | This study |
| VS1667-11B | *h- ade6-M210 ura4-D18 his3-D1 kanMX6-Pnmt1-3x-act1 leu1-32::Pact1-LifeAct-GFP-leu1+* | This study |
| VS1820-9D | *h? ade6-M216 ura4-D18 his3-D1 natMX4-3xPnmt1-cdc3 kanMX6-Pnmt1-3x-act1 leu1-32::Pact1-LifeAct-GFP-leu1+* | This study |

**Table S2. Fission yeast strains used in this study, related to Experimental Procedures.** All of the strains used in this study are listed, including their names and genotypes.

## SUPPLEMENTAL MOVIE DESCRIPTIONS

**Movie S1. Endocytic actin patches in profilin mutant cdc3-124 cells, related to Figures 2A–2C.** Fluorescent time lapse images of Lifeact-mCherry labeled actin patches in WT, *cdc3-124*, or *cdc3-124* cells expressing SpPRF, SpPRF(Y5D), or SpPRF(K81E) cells at 36˚C. Representative normal (yellow) and aberrant (red) patches are marked with arrows. Scale bar, 2 μm. Time in sec.

**Movie S2. Profilin inhibits Arp2/3 complex-mediated actin assembly *in vitro*, related to Figures 3A and 3B.** TIRFM visualization of the assembly of 1.5 μM Mg-ATP-actin (15% OG-actin) with 40 nM SpArp2/3 complex and 80 nM SpWsp1(VCA) in the absence of profilin (left), presence of 5 μM profilin SpPRF (middle), or presence of 10 pM formin SNAP-549(red)-Cdc12(FH1$^{1P}$FH2) and 5 μM SpPRF (right). Scale bar 2 μm. Time in min:sec.

**Movie S3. Profilin favors formin- over Arp2/3 complex-mediated actin assembly *in vitro*, related to Figures 4A–4D.** TIRFM visualization of the assembly of 1.5 μM Mg-ATP-actin (15% OG-actin) with 40 nM Arp2/3 complex, 80 nM SpWsp1(VCA), and 100 pM formin SNAP-549(red)-SpCdc12(FH1$^{1P}$FH2). At t = 0 sec additional Arp2/3 complex and SpWsp1(VCA) were flowed into the chamber in the absence (left) or presence of 5 μM WT SpPRF (right). Scale bar 2 μm. Time in sec.

**Movie S4. Profilin inhibits Arp2/3 complex-mediated actin assembly from beads, related to Figures 5A–5E.** TIRFM visualization of the assembly of 1.5 μM G-actin from GST-pWA-coated beads. Initial reactions contained 1.5 μM G-actin (10% TMR-actin) and 10 nM mArp2/3 complex. At t = 0 sec, 1.5 μM actin (15% Oregon green-actin) was flowed into the reaction chamber with 10 nM mArp2/3 complex in either the absence (left) or presence of 5 μM WT SpPRF (right). Oregon green-actin was bleached twice to reveal new assembly from the bead surface. Scale bar, 2 μm. Time in sec.

**Movie S5. Profilin favors formin- over Arp2/3 complex-mediated actin assembly from beads, related to Figures 5F-5H.** TIRFM visualization of the assembly of 1.5 μM G-actin from a mixture of GST-pWA- and formin SNAP-mDia2(FH1FH2)-coated beads. Initial reactions contained 1.5 μM G-actin (10% TMR-actin) with 2 nM mArp2/3 complex. At 240 seconds, 1.5 μM G-actin (15% OG-actin) with 2 nM mArp2/3 complex and 5 μM SpPRF was flowed into the chamber. Scale bars, 2 μm. Time in sec.

## SUPPLEMENTAL EXPERIMENTAL PROCEDURES

### Plasmid construction

Fission yeast formin SNAP-SpCdc12(FH1$^{1P}$FH2) (residues 927-1390), which contains one of two profilin-binding proline-rich regions in the FH1 domain (Scott et al., 2011), and mammalian formin SNAP-mDia2(FH1FH2) (residues 521-1171) were prepared following PCR amplification (iProof, Bio-Rad, Hercules, CA) by using In-Fusion kit (Clontech) or by subcloning into SNAP-tag-T7-2 vector (New England Biolabs) at the XmaI/PacI sites. A flexible linker (GGSGGS) was included in the forward primer, and 6His tag for purification was included in the reverse primer, of all SNAP constructs. Full-length SpWsp1 ORF or SpWsp1-VCA were amplified from Wsp1 cDNA generated by RT-PCR and subcloned into EcoR1 and BamH1 sites of pGEX-2 and pGEX-6 (GE Life Sciences, Piscataway, NJ), to generate N-terminal GST fusions. Full-length SpWsp1 ORF or SpWsp1-VCA were amplified from Wsp1 cDNA generated by RT-PCR and subcloned into EcoR1 and BamH1 sites of pGEX-2 and pGEX-6 (GE Life Sciences, Piscataway, NJ), to generate N-terminal GST fusions.

### Protein expression and purification

Actin was purified from rabbit skeletal-muscle acetone powder (Spudich and Watt, 1971) and labeled on Cys374 with pyrenyliodoacetamide (Cooper et al., 1983), Oregon Green iodoacetamide (Kuhn and Pollard, 2005), or Tetramethylrhodamine-6-maleimide (TMR) (Kudryashov and Reisler, 2003). WT fission yeast profilin SpPRF, mutant SpPRF(K81E) and human profilin HPRO1 were overexpressed and purified from *Escherichia coli* by poly-L-proline affinity chromatography (Ezezika et al., 2009; Lu and Pollard, 2001). Mutant profilin SpPRF(Y5D) was overexpressed and purified from bacteria by biochemical fractionation (Lu and Pollard, 2001). Arp2/3 complex was purified from *S. pombe* (Arp2/3 complex) or calf thymus (mArp2/3 complex) by WASp(VCA) affinity chromatography (Egile et al., 1999; Sirotkin et al., 2005). WASP fragment constructs fission yeast GST-Wsp1(VCA) and GST-human WASp pWA were purified by Glutathione-Sepharose affinity chromatography (Achard et al., 2010; Higgs et al., 1999; Sirotkin et al., 2005). Mouse capping protein (CP) was purified from bacteria (Palmgren et al., 2001).

Full length fission yeast WASp GST-Wsp1(FL) was overexpressed in *Escherichia coli* strain BL21-Codon Plus (DE3)-RP (Stratagene) grown in LB media plus 0.1 mg/ml ampicillin and induced overnight at 16˚C with 500 μM IPTG. Cells were centrifuged at 10,000 rpm for 15 minutes, and then re-suspended in GST-Extraction buffer (20 mM Tris pH 8.0, 100 mM NaCl, 2 mM EDTA, 2 mM DTT, 500 μM PMSF, 10 μg/ml leupeptin/pepstatin A). After lysis with an Emulsi-Flex-C3 (Avestin), cells were centrifuged at 18,000 rpm for 45 minutes. Proteins were incubated with Glutathione-Sepharose resin (GE Healthcare) for 1 hour at 4˚C, and loaded onto a column. The resin was rinsed with 80 ml GST-wash buffer (20 mM Tris pH 8.0, 100 mM NaCl, 2 mM EDTA, 2 mM DTT), and proteins were eluted with GST-Elution buffer (50 mM Tris pH 8, 100 mM NaCl, 1 mM DTT, 50 mM reduced Glutathione). Fractions containing the protein were dialyzed overnight with SA buffer (10 mM HEPES pH 7.2, 50 mM NaCl, 5% glycerol, 10% $NaN_3$, 2 ml DTT) and then loaded onto a 1 ml HiTrap$^{TM}$ SP column (GE Healthcare). GST-Wsp1(FL) was eluted with a 0.05-1M gradient of SB Buffer (10 mM HEPES pH 7.2, 1 M NaCl, 5% glycerol, 10% $NaN_3$, 2 ml DTT). Fractions containing GST-Wsp1(FL) were gel filtered and stored at -80˚C in 20 mM Tris pH 8.0, 250 mM NaCl, 1 mM DTT. The concentration of GST-Wsp1(FL) was determined by densitometry of Coomassie-stained bands on SDS/PAGE gels compared with actin standards.

Fission yeast formin SNAP-SpCdc12(FH1$^{1P}$FH2) and mammalian formin SNAP-mDia2(FH1FH2) tagged with a His-Tag at the C-terminus were expressed in *Escherichia coli* strain BL21-Codon Plus (DE3)-RP with 500 μM IPTG overnight at 16°C. Cells were lysed in formin extraction buffer (50 mM $NaH_2PO_4$, pH 8.0, 500 mM NaCl, 10% glycerol, 10 mM imidazole, 10 mM β-mercaptoethanol, 500 μM PMSF, 10 μg/ml leupeptin/pepstatin A), and clarified. Proteins were incubated with Talon Resin for 1 hour at 4˚C then loaded onto a column. The resin was rinsed with 80 ml wash buffer (50 mM $NaH_2PO_4$ pH 8.0, 500 mM NaCl, 10% glycerol, 10 mM imidazole, 10 mM β-mercaptoethanol), and proteins were eluted with 250 mM imidazole in wash buffer. Fractions containing the protein were dialyzed overnight with QA buffer (20 mM Tris pH 8.0, 100 mM NaCl, 1 mM DTT) and loaded onto a 1 ml HiTrap$^{TM}$ HP column. SNAP-tagged proteins were eluted with a gradient of 0.1-1M NaCl in QB buffer (20 mM Tris pH 8.0, 1 mM DTT). Fractions containing SNAP-tagged proteins were stored at -80˚C in 20 mM Hepes, pH 7.4, 200 mM KCl, 0.01% $NaN_3$, 1 mM DTT, and 10 % glycerol. SNAP-SpCdc12(FH1$^{1P}$FH2) was labeled with SNAP-Surface$^{TM}$549 following manufacturer's protocol

(New England Biolabs, Ipswich, MA). Labeled SNAP-549(red)-SpCdc12(FH1$^{1P}$FH2) was stored at -80˚C in 20 mM Hepes, pH 7.4, 200 mM KCl, 0.01% $NaN_3$, 1 mM DTT, and 10% glycerol. Concentrations of SNAP-tagged proteins and percent labeling were determined by measuring fluorophore absorbance in solution using the extinction coefficients SNAP-Surface$^{TM}$549: $\varepsilon_{560}$ = 150,000 M/cm.

**Quantitative immunoblotting of actin and profilin levels**

Actin and profilin over-expression cells were grown overnight in YE5S at 25°C, washed three times with EMM5S without thiamine, re-seeded into EMM5S without thiamine, grown at 25°C for 22 hrs, and harvested by centrifugation. Cells were disrupted by glass bead lysis in a FastPrep-24 (MP Biomedicals, Solon, OH) in Lysis Buffer U (50 mM Hepes, pH 7.5, 100 mM KCl, 3 mM $MgCl_2$, 1 mM EGTA, 1 mM EDTA, 0.1% Triton X-100, 1 mM DTT, 1 mM PMSF, and Complete protease inhibitors (Roche, Fishers, IN). Samples were separated on SDS-PAGE gels and transferred onto PVDF membranes. Actin was detected by immunoblotting with anti-actin C4 monoclonal antibody (Sigma, St. Louis, MO) and secondary HRP-conjugated anti-mouse IgG antibody with SuperSignal West-Dura ECL reagent (Thermo-Pierce, Rockford, IL). Profilin was detected with rabbit anti-profilin polyclonal antibodies (Lu and Pollard, 2001) and secondary HRP-conjugated anti-rabbit IgG antibodies.

Actin and profilin levels in samples of wild type and overexpressing cells were quantified in Image Lab (Bio-Rad, Hercules, CA) from images of blots in the linear range of serial dilutions of cell extracts or purified proteins. All samples were prepared from known numbers of cells calculated from optical density (at 595 nm) of cell cultures. Wild type actin and profilin levels were quantified from images of blots of wild type cell extracts and serial dilutions of purified chicken skeletal muscle actin and profilin SpPRF at known concentrations. The level of overexpression of actin and profilin were quantified from images of blots of wild type cell extracts and serial dilutions of extracts from overexpessing cells. Cytoplasmic concentrations were then calculated from the number of molecules per cell and average cytoplasmic volume as described (Wu and Pollard, 2005).

**Anisotropy**

Anisotropy measurements were made with a Tecan Safire II (Tecan, Durhnam, NC) plate reader. 100 nM Rhodamine-labeled TMR-SpWsp1-VCA was mixed with a range of concentration of actin alone or in the presence of 20 μM WT profilin SpPRF (Marchand et al., 2001). TMR was excited with polarized light at 530 nm and the emitted light was detected at 576 nm through both horizontal and vertical polarizers. Dissociation-equilibrium constants (Kd) were calculated by fitting equation (1) to the ligand-concentration dependence of the anisotropy (Vinson et al., 1998).

$$r = r_f + (r_b - r_f)\frac{\left(K_d + [W] + [A] - \sqrt{(K_d + [W] + [A])^2 - (4[W][A])}\right)}{2[W]} \qquad (1)$$

where $r_f$ is the anisotropy value of free TMR-SpWsp1-VCA, $r_b$ is the anisotropy of TMR-SpWsp1-VCA bound to actin, [W] is the concentration of TMR-SpWsp1-VCA, and [A] is the concentration of actin.

For fluorescent anisotropy competition experiments between SpPRF and TMR-SpWsp1-VCA for binding actin, data were fitted to the equation (2) (Vinson et al., 1998).

$$r = r_f + (r_b - r_f)/\left[(K_d([P] + K_2)/K_2[A]) + 1\right] \qquad (2)$$

where $K_d$ is the dissociation-equilibrium constant of labeled TMR-SpWsp1-VCA binding to actin, [A] is the total concentration of actin, [P] is the concentration of SpPRF, and $K_2$ is the $K_d$ of SpPRF for binding actin (Lu and Pollard, 2001).

**Pull down assay**

2.0 μM GST-Wsp1-VCA was immobilized on Glutathione-Sepharose beads and incubated with 0.3 μM SpArp2/3 complex in the absence and presence of 58 μM WT profilin SpPRF. Quantification of bound and unbound Arp2/3 complex were measured by gel densitometry on an Odyssey Infrared Imager (LI-COR Biosciences, Lincoln, NE).

## SUPPLEMENTAL REFERENCES


Achard, V., Martiel, J.L., Michelot, A., Guerin, C., Reymann, A.C., Blanchoin, L., and Boujemaa-Paterski, R. (2010). A "primer"-based mechanism underlies branched actin filament network formation and motility. Curr Biol *20*, 423-428.

Burke, T.A., Christensen, J.R., Barone, E., Suarez, C., Sirotkin, V., and Kovar, D.R. (2014). Homeostatic Actin Cytoskeleton Networks Are Regulated by Assembly Factor Competition for Monomers. Curr Biol *24*, 579-85.

Chang, F., Drubin, D., and Nurse, P. (1997). cdc12p, a protein required for cytokinesis in fission yeast, is a component of the cell division ring and interacts with profilin. J Cell Biol *137*, 169-182.

Cooper, J.A., Walker, S.B., and Pollard, T.D. (1983). Pyrene actin: documentation of the validity of a sensitive assay for actin polymerization. J Muscle Res Cell Motil *4*, 253-262.

Egile, C., Loisel, T.P., Laurent, V., Li, R., Pantaloni, D., Sansonetti, P.J., and Carlier, M.F. (1999). Activation of the CDC42 effector N-WASP by the Shigella flexneri IcsA protein promotes actin nucleation by Arp2/3 complex and bacterial actin-based motility. J Cell Biol *146*, 1319-1332.

Ezezika, O.C., Younger, N.S., Lu, J., Kaiser, D.A., Corbin, Z.A., Nolen, B.J., Kovar, D.R., and Pollard, T.D. (2009). Incompatibility with formin Cdc12p prevents human profilin from substituting for fission yeast profilin: insights from crystal structures of fission yeast profilin. J Biol Chem *284*, 2088-2097.

Higgs, H.N., Blanchoin, L., and Pollard, T.D. (1999). Influence of the C terminus of Wiskott-Aldrich syndrome protein (WASp) and the Arp2/3 complex on actin polymerization. Biochemistry *38*, 15212-15222.

Huang, J., Huang, Y., Yu, H., Subramanian, D., Padmanabhan, A., Thadani, R., Tao, Y., Tang, X., Wedlich-Soldner, R., and Balasubramanian, M.K. (2012). Nonmedially assembled F-actin cables incorporate into the actomyosin ring in fission yeast. J Cell Biol *199*, 831-847.

Kovar, D.R., Wu, J.Q., and Pollard, T.D. (2005). Profilin-mediated competition between capping protein and formin Cdc12p during cytokinesis in fission yeast. Mol Biol Cell *16*, 2313-2324.

Kudryashov, D.S., and Reisler, E. (2003). Solution properties of tetramethylrhodamine-modified G-actin. Biophys J *85*, 2466-2475.

Kuhn, J.R., and Pollard, T.D. (2005). Real-time measurements of actin filament polymerization by total internal reflection fluorescence microscopy. Biophys J *88*, 1387-1402.

Lord, M., and Pollard, T.D. (2004). UCS protein Rng3p activates actin filament gliding by fission yeast myosin-II. J Cell Biol *167*, 315-325.

Lu, J., and Pollard, T.D. (2001). Profilin binding to poly-L-proline and actin monomers along with ability to catalyze actin nucleotide exchange is required for viability of fission yeast. Mol Biol Cell *12*, 1161-1175.

Marchand, J.B., Kaiser, D.A., Pollard, T.D., and Higgs, H.N. (2001). Interaction of WASP/Scar proteins with actin and vertebrate Arp2/3 complex. Nat Cell Biol *3*, 76-82.

McCollum, D., Balasubramanian, M.K., Pelcher, L.E., Hemmingsen, S.M., and Gould, K.L. (1995). Schizosaccharomyces pombe cdc4+ gene encodes a novel EF-hand protein essential for cytokinesis. J Cell Biol *130*, 651-660.

Nurse, P., Thuriaux, P., and Nasmyth, K. (1976). Genetic control of the cell division cycle in the fission yeast Schizosaccharomyces pombe. Mol Gen Genet *146*, 167-178.

Palmgren, S., Ojala, P.J., Wear, M.A., Cooper, J.A., and Lappalainen, P. (2001). Interactions with PIP2, ADP-actin monomers, and capping protein regulate the activity and localization of yeast twinfilin. J Cell Biol *155*, 251-260.

Scott, B.J., Neidt, E.M., and Kovar, D.R. (2011). The functionally distinct fission yeast formins have specific actin-assembly properties. Mol Biol Cell *22*, 3826-3839.

Sirotkin, V., Beltzner, C.C., Marchand, J.B., and Pollard, T.D. (2005). Interactions of WASp, myosin-I, and verprolin with Arp2/3 complex during actin patch assembly in fission yeast. J Cell Biol *170*, 637-648.

Spudich, J.A., and Watt, S. (1971). The regulation of rabbit skeletal muscle contraction. I. Biochemical studies of the interaction of the tropomyosin-troponin complex with actin and the proteolytic fragments of myosin. J Biol Chem *246*, 4866-4871.

Vinson, V.K., De La Cruz, E.M., Higgs, H.N., and Pollard, T.D. (1998). Interactions of Acanthamoeba profilin with actin and nucleotides bound to actin. Biochemistry *37*, 10871-10880.

Wu, J.Q., and Pollard, T.D. (2005). Counting cytokinesis proteins globally and locally in fission yeast. Science *310*, 310-314.